

NUMERICAL AND ANALYTICAL STUDIES OF JOINT COMPONENT BEHAVIOUR IN FIRE

Florian M. BLOCK¹, Ian W. BURGESS and J. Buick DAVISON

*University of Sheffield, Mappin Street, Sheffield S1 3JD, United Kingdom
(¹cip02fmb@sheffield.ac.uk)*

ABSTRACT

Full-scale fire tests have clearly shown that joints in composite steel-frame buildings have a considerable effect on the survival time of the structure, due to their ability to transfer forces from hot parts of the structure to cooler zones. Realistic modelling of joints in global analysis could be of great importance in structural fire design calculations, which can either be used to give confidence about safety margins or to help to reduce the cost of fire protection strategies. A versatile approach for predicting the high temperature behaviour of joints is the “Component Method”, in which a joint is considered as an assembly of a number of individual basic components, allowing a large number of possible variables in a beam-to-column joint to be considered simultaneously. This method provides a practical analytical approach to joint modelling under the simultaneous effects of loading, thermal degradation of materials and forces due to restraint of thermal expansion, all of which occur concurrently in a building fire. This paper describes the main findings from an ongoing study of the column web compression zone in fire, including the effect of superstructure loading. A range of column sections has been analysed at different temperatures and axial load ratios under transverse loading using *ANSYS*. From this study a temperature-dependent reduction factor for the transverse resistance of the column web and a simplified analytical approach have been developed to predict the force-displacement behaviour of the compression zone. The results have been compared with high temperature experiments and generally good correlation has been found. The test setup for a further series of bi-axial high temperature compression experiments is described.

KEYWORDS: *Structural fire engineering, steel joints, component method, compression zone, axial load, high temperature experiments*

INTRODUCTION

In the past 20 years considerable progress has been made in the parallel research fields of the behaviour of semi-rigid steelwork connections and structural fire engineering of steel-framed buildings. Bringing these themes together it should be possible to develop safe and economic design methods for the fire-resistance of steel frames, using the semi-rigid nature of their connections in fire. Because of the large number of possible variables in the detailed design of a semi-rigid beam-to-column connection, a versatile approach for calculating the rotational stiffness and load capacity of connections was developed in the European research project COST Action C1, and its results have been introduced into the draft Eurocode EC3 Part 1.8 [1]. The original feature of this “Component Method” is to consider any joint as a set of individual basic components. In the particular case of Fig. 1, which illustrates an external beam-to-column joint using an extended end-plate connection subject to moment, the joint is divided into the three major zones (tension, shear and compression), and then each zone is divided into the relevant components.

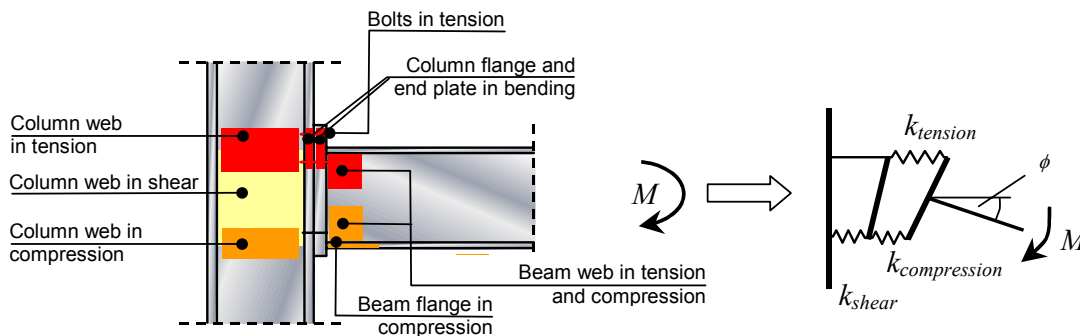


FIGURE 1 : Components of a beam-to-column joint and a simple spring model (EC3)

For each component the stiffness and maximum load is computed and assembled to form a spring model, which gives the rotational behaviour of the whole connection. Recent research [2] has shown that the compression zone in the column web is the critical component from the three zones in the connection if rotational capacity is needed, due to its limited ductility. In composite connections this zone becomes more critical because of the stronger tension zone produced by continuing slab reinforcement.

In a building fire the compression zone becomes even more critical because of restraint to the thermal expansion of the steel beams, which causes large compressive forces in the column web. Full-scale fire tests and accidental fires have clearly shown that joints have a considerable effect on the survival time of the structure because they may occur at interfaces at which forces from a hot part of the structure react against cooler zones. Considering this, realistic modelling of joints in global analysis could be of great importance in structural fire design calculations, which can either be used to give confidence about safety margins or to help to reduce the cost of fire protection strategies.

EXISTING DESIGN APPROACHES FOR THE COMPRESSION ZONE

This paper concentrates on the compression zone in the column web. To find the resistance of the compression zone at elevated temperatures, it is logical to use a proven approach for ambient temperatures and to apply the well-established strength reduction factors adopted in EC3 Part 1.2 [3] to it to simulate fire conditions. In order to find the most accurate equation for the ultimate load at ambient temperature, different design approaches have been compared with the results of 64 tests on the compression zone in column webs of European

and British rolled sections conducted by Aribert [4], Spyrou [5] and Kühnemund [2]. Most of the design approaches are conservative and give erratic correlation with the ultimate loads found in the experiments. The majority of the reported tests were conducted with two opposed transverse loads introduced through the flanges, but the co-existent axial force present in a real column has been neglected. Only Kühnemund considered the influence of the axial force in the column. A statistical comparison of the approaches has been conducted by the author [6] and it was found that the approach of Lagerqvist and Johansson [7] yielded the most accurate results with a reasonable margin of safety. This approach was used to predict the opposed patch-load tests at elevated temperatures conducted at the University of Sheffield by Spyrou [5] and good agreement was found.

In order to describe joint behaviour realistically a full force-displacement curve for each component is needed, therefore an empirical equation for the displacement at the peak load of the compression zone has been developed based on a parametric study of finite element models and test results. To describe the path up to the peak load the classical Ramberg-Osgood equation was modified. An example of the correlation between the analytical model and high-temperature test results is shown in Fig. 2 below.

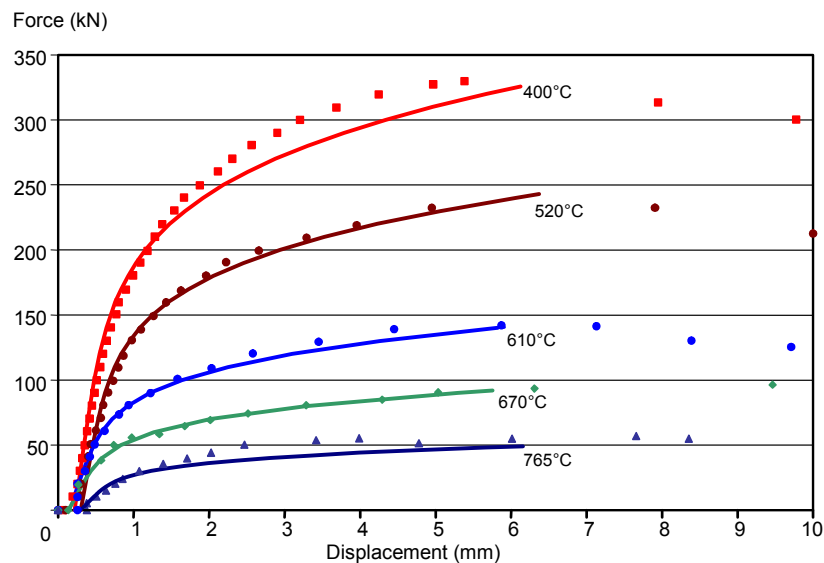


FIGURE 2 : F- δ curves of a UC 203x203x46 from tests and the new approach

From Fig. 2 it can be seen that the new approach predicts the test results very accurately. Similar good correlation was found in other experiments. The displacement at ultimate load is predicted conservatively at very high temperatures. However, the analytical model does not at present consider the influence of axial load in the column, and the current work aims to predict this influence at elevated temperatures.

THE INFLUENCE OF AXIAL LOADING ON THE COMPRESSION ZONE

Experimental research projects at different European research centres on full joint assemblies and single components have shown that the ductility as well as the ultimate resistance force of the compression zone is reduced by the presence of axial-stress in the column. Probably the first attempt to quantify the effects was made by Zoetemeijer [8] in 1975. Together with an effective-width approach for the yield load of the compression zone under opposed patch loading he developed from tests a transverse resistance reduction factor

k_{wc} for cases where the longitudinal stress in the column web is larger than 50% of its yield stress. The factor k_{wc} can be calculated from

$$k_{wc} = 1.25 - 0.5 \frac{\sigma_{com,Ed}}{f_{y,wc}} \quad (1)$$

where $\sigma_{com,Ed}$ is the longitudinal stress in the column web and $f_{y,wc}$ is the yield stress of the column web. This equation has been adopted in EC3 Part 1.8 and is calibrated for the effective width approach. Ahmed and Nethercot [9] applied the von Mises yield theory to the problem and concluded that no reduction factor is needed for bi-axial compression in the column web. Bailey and Moore [10] differentiated between yielding and buckling failure modes, and used the von Mises yield theory with an imperfection factor and elastic stability equations respectively to develop reduction factors for the maximum capacity of the column web. The reduction factor for yielding failure is given in Table 1, in which σ_N is the normal stress in the web and f_y the yield stress of the web.

σ_N / f_y	$k_{wc,yield}$
≤ 0.7	1.0
0.8	0.95
0.9	0.85
1.0	0.7

Table 1 : Reduction factor according to Bailey and Moore for yielding mode.

For buckling problems they recommend the use of

$$k_{wc,buck} = \left(1 - \frac{F_{axial}}{F_{cr(axial)}} \right) \quad (2)$$

where F_{axial} represents the axial force in the column and $F_{cr(axial)}$ its load carrying capacity. Kühnemund [2] used a different reduction factor to account for the effects of axial stresses. This factor had first been derived by Djubek and Skaloud [11] in the context of reduction of the transverse load capacity due to bending stresses in plate girders as

$$k_N = \sqrt{1 - \left(\frac{\sigma_N}{f_y} \right)^2} \quad (3)$$

These three equations are shown in Fig. 3 below.

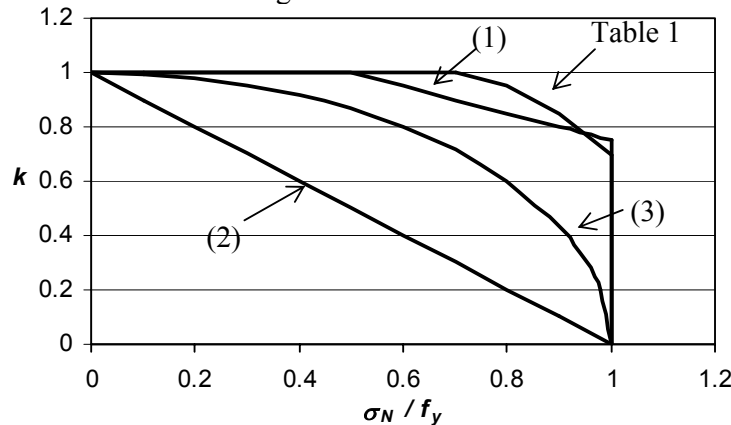


FIGURE 3 : Axial load reduction factors

FINITE ELEMENT STUDY

In order to investigate whether one of the existing reduction factors can be used to account for the effect of axial stress in the column at elevated temperatures some finite element studies have been conducted on three different British Universal Column (UC) sections, of sizes UC152x152x37, UC203x203x46 and UC305x305x167. A range of temperatures from 20°C to 650°C, and axial stress levels from 0% to 80% of the yield stress at the relevant temperatures, have been investigated. The sections have been chosen to cover a range of web slenderness, with d/t values from 22.3 to 10.4. A mixed 2D - 3D shell model was used, in which the flanges of the column section were very thick shell elements in-line with the web, so it was possible to model the spread of stress through the flanges into the web, using shell elements to model the stability and out-of-plane bending effects in the web. In contrast to a model employing solid elements, the chosen way of modelling is very economic in terms of computing time and hard disk space, because in a solid model the thickness of the web needs to be divided into a large number of elements to enable buckling to be modelled adequately. This was shown by Tryland *et al.* [12]; the stress distribution in the web of the hybrid model was compared with a solid element model and little difference could be found. Rolled sections are never perfectly straight and therefore an imperfection in the web (according to the first eigenvalue shape) has been introduced as

$$y = \sin\left(\frac{n_1\pi}{l}x\right)\sin\left(\frac{n_2\pi}{h}z\right)\frac{d}{500} \quad (4)$$

where n_1 and n_2 are the half-waves in the x and z directions respectively; h and l are the distance between the root radii and the length of the model. A picture of a typical model is shown in Fig. 4, in which the amplitude of the imperfection is scaled by a factor of 10 to make the shape more visible. The thicknesses of shell elements are shown and the root radius approximation be seen.

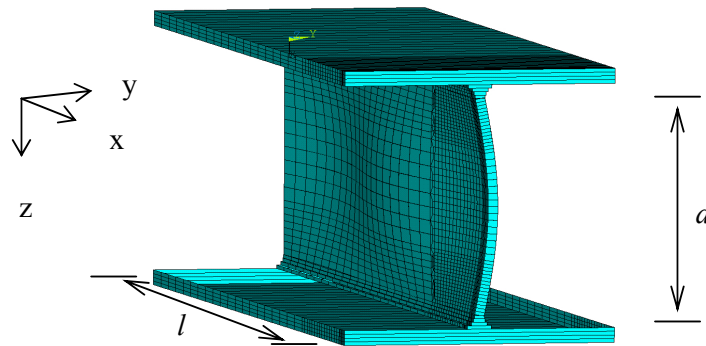


FIGURE 4 : Typical mesh and imperfection of the compression zone

In the cases where axial load is included it is introduced at the end of the section, and the boundary at the centre of the transverse load patch has restraint conditions appropriate to an axis of symmetry. To guarantee a uniform distribution of the axial load across the section the nodes on which the forces are applied are coupled in the loading direction. The material used in the models is S275 steel with a Young's modulus of 205000 N/mm², a yield stress of 275 N/mm² and an ultimate strength of 455 N/mm². To include the effect of elevated temperature in the analysis, a uniform temperature distribution through the cross-section has been assumed and the stress-strain curve for steel according to the recommendations in EC3 Part 1.2 has been used.

At ambient temperature the model for the stress-strain curve including strain hardening published by Zheng *et al.* [13] has been used. The tangent modulus of the strain hardening part of the curve can be expressed as

$$E' = E_{st} \exp\left(-\xi \frac{\varepsilon - \varepsilon_{st}}{\varepsilon_y}\right) \quad (5)$$

where E is the elastic modulus; ε_y is the yield strain; ε_{st} is the strain at the onset of strain hardening, taken as $10\varepsilon_y$; E_{st} is the initial strain hardening modulus taken as $E/40$ and E' is the assumed strain hardening modulus. The factor ξ is calibrated to reach the ultimate stress at a strain of 20%. The analysis is divided into two steps: firstly axial loading of the specimen, and secondly the application of transverse load until the peak load is reached and stability failure of the web occurs, leading to post-buckling behaviour. This last part of the behaviour is important when large rotations of the beam ends are expected, as tends to happen in fire conditions.

A comparison with experimental results [5] at ambient and elevated temperatures for transverse loading only and the finite element model described above shows a good correlation as illustrated in Fig. 5 below.

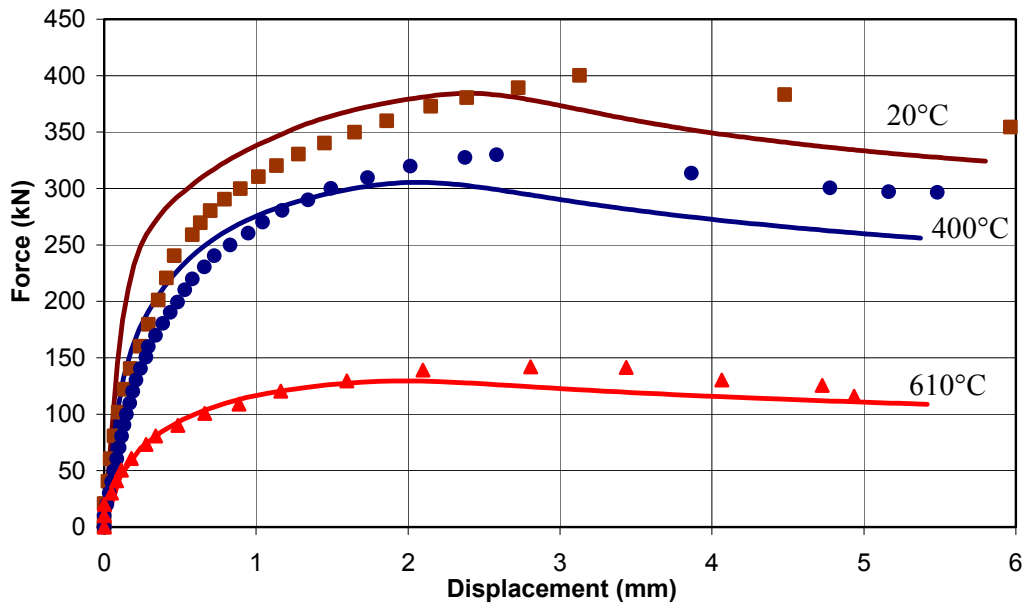


FIGURE 5 : Experimental and numerical results without axial load

Good correlation between numerical and experimental results can be seen in the initial part, but when the load increases the model is weaker, and fails about 10% lower than the tests. This could be due to lower temperatures in the core of the tested section and therefore larger residual material strength. Also the temperature reduction factors account for the effects of thermal creep, which are not present in the steady-state experiments used, due to the testing speed. The creep effects are known to decrease the strength and stiffness of steel by about 8% to 9%. Furthermore, in the EC3-1.2 stress-strain curves no strain hardening effects are considered above 400°C but strain hardening has a significant influence on the capacity of the section, because of the fairly large strains occurring directly under the transverse load and in the plastic hinges.

The study was extended to bi-axial loading. A typical set of force – displacement curves is shown in Fig. 6 below.

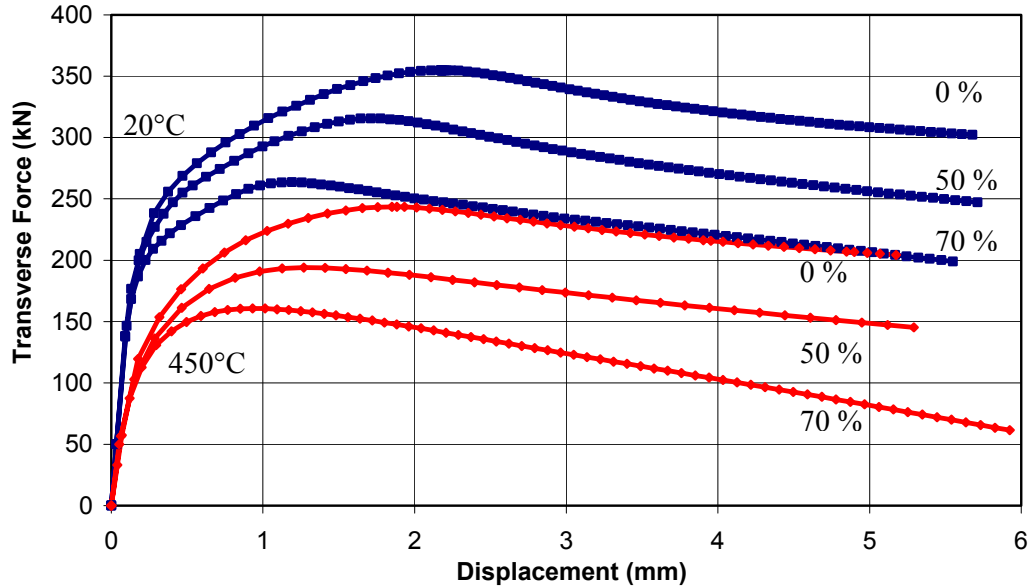


FIGURE 6 : Transverse force-displacement for UC 203x203x46 at 20°C and 450°C under axial loads 0% - 70% of yield.

From the force-displacement curves plotted in Fig. 6 a significant reduction of the capacity and the ductility of the compression zone is apparent in the presence of axial load. This reduction increases as temperatures increase, due to the decrease of the proportional limit of the stress-strain curve and therefore reduced tangent modulus at low stress levels. Furthermore, the missing strain-hardening at temperatures above 400°C changes the post-peak behaviour of the column web. Whereas at ambient temperature, even for high axial load levels, the web behaviour recovers slightly due to membrane effects after the peak load, at elevated temperatures no membrane effects can be developed in the highly strained areas due to the lack of strain-hardening. Hence, under high axial loads the post peak behaviour decreases rapidly because of the second-order effects in the buckled column web introduced by the axial load. In Fig. 7 the interaction of the normalised peak loads (R/R_T) and the normalised axial forces (N/N_{pl}) are shown for all 45 analyses.

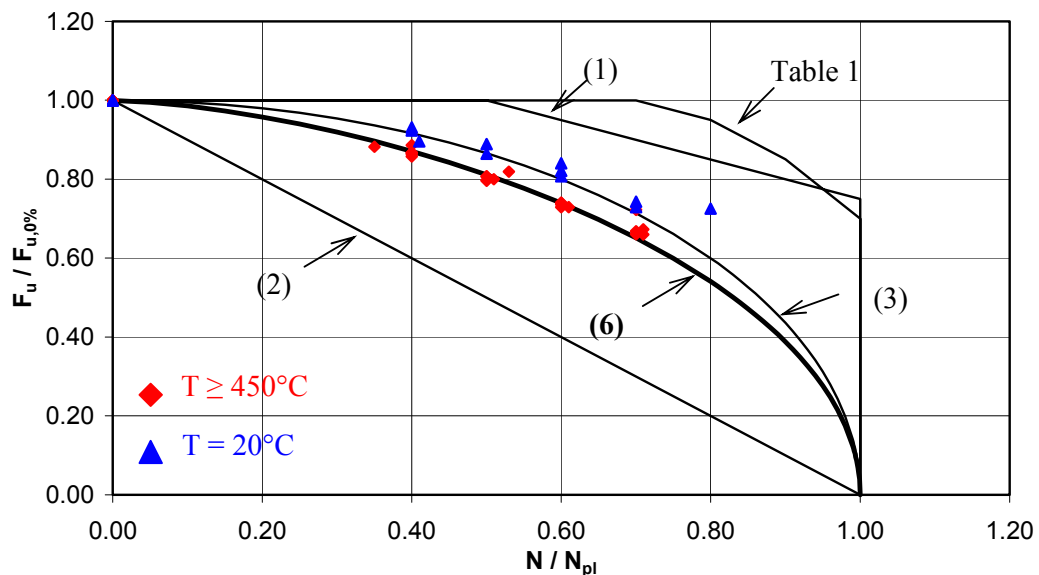


FIGURE 7 : Reduction of the peak load due to axial loads in the column

Details of the analyses are shown in the Appendix. For each section at each temperature the peak loads are normalised with respect to the peak load under zero axial load and the axial load to the yield load of the section using the yield stress at the relevant temperature.

It is remarkable that both the ambient- and elevated-temperature sets of results ($T=20^{\circ}\text{C}$, $T>450^{\circ}\text{C}$) show similar behaviour, which suggests that the change in the style of the stress-strain curve has a larger influence on the peak load reduction than the different temperatures. Furthermore, the different approaches for the reduction factors given in the literature are shown in Fig. 7 and it becomes quite clear that only equation (3) gives reasonable results for the ambient temperature cases, but at the higher temperatures which occur in a protected column exposed to fire a rather larger reduction factor should be used. Until an analytical equation has been developed the following approach can be used:

$$k_N = \sqrt{1 - \left(\frac{\sigma_N}{k_{y,t} f_{y,w}} \right)^{1.55}} \quad (6)$$

where σ_N is the longitudinal stress in the column web; $k_{y,t}$ is the temperature-dependent yield strength reduction factor given in EC3 and $f_{y,w}$ the yield stress of the column web.

Referring back to Fig. 6, the displacements associated with the peak load are reduced by the influence of the axial force in the column. To make this reduction more visible the displacements at peak load are normalised against those under zero axial load for each set of temperatures and section sizes. This reduction is shown in Fig. 8.

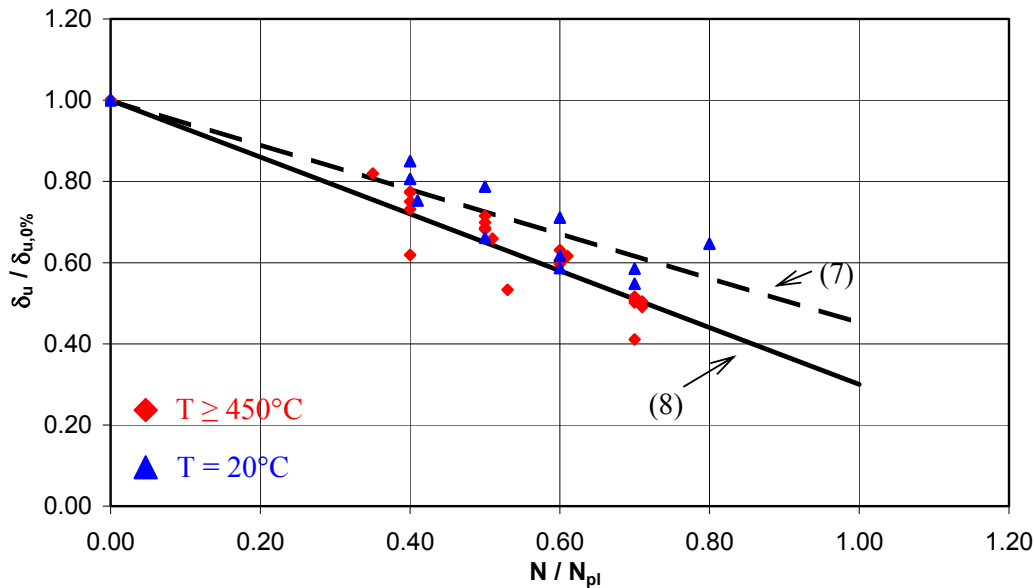


FIGURE 8 : Reduction of the peak displacement due to the presence of axial load

For this phenomenon no reduction factor has been published to date, but it is important to know this factor if the full force-displacement curve for the component is to be predicted. Linear equations based on a regression calculation can be proposed which represent the mean peak load reduction factor. The first, for ambient temperature behaviour, is

$$k_{N,\delta,20^{\circ}\text{C}} = -0.55 \frac{\sigma_N}{f_y} + 1 \quad (7)$$

and for temperatures above 400°C ,

$$k_{N,\delta,\geq 400^\circ C} = -0.70 \frac{\sigma_N}{f_y} + 1 \quad (8)$$

Using the above reduction factors it is possible to extend the simplified approach for the compression zone to include the effect of axial load in the column. As an example the results from the numerical analysis of the UC 203x203x46 at 450°C and 650°C for axial load levels of 0%, 50% and 70% are shown in Fig. 9, together with analytical results based on the simplified method presented in [6].

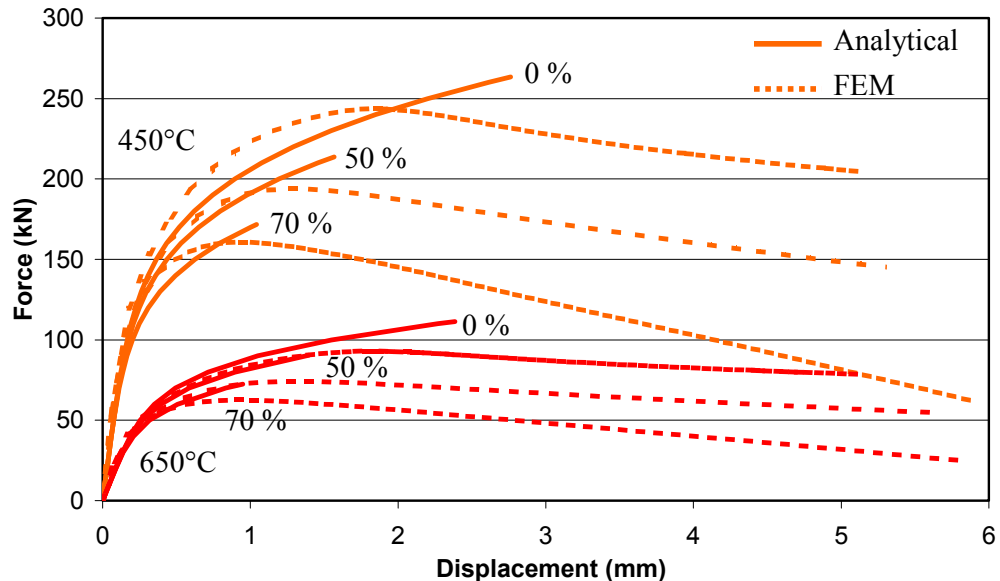


FIGURE 9 : Comparison of simplified prediction with FEM results for UC203x203x46.

In similar fashion to the comparison with experiments given in Fig. 5 the numerically calculated curves show weaker behaviour than the analytical approach, but in general a good correlation can be seen.

EXPERIMENTAL STUDIES

An experimental study is due to start in April 2004 in order to validate the finite element analysis of the column web under bi-axial loading at elevated temperatures. A British universal column section (UC 152x152x37) is to be tested in a horizontal position. The experimental set-up consists of three major parts. A horizontal loading device, which includes a hydraulic jack attached via a pressure-controlled pump to a reaction frame, applies the axial force. The role of the pressure-control system is to keep the axial load constant as the specimen expands due to its increasing temperature (see Fig. 10a). An electrically-heated furnace box wraps around the column section, which protrudes through shaped holes in removable panels at both ends. The furnace is insulated with 50mm fibre-board and uses commercial electric heating elements, closely arranged around the specimen. The elements have a total power rating of 8kW. Each of the six elements can be controlled separately to achieve a uniform heating profile in the column section (see Fig. 10b). A vertical loading device consisting of a displacement-controlled actuator attached to the reaction frame applies the transverse compression to the section. To simulate the beam flanges in an internal joint this transverse load is introduced via steel plates of 20mm thickness with rounded edges. These plates can be moved out of the furnace to prevent them from becoming overheated (see Fig. 10c). To allow for the vertical movement of the centre-line of the specimen, which

occurs when the transverse load is applied, roller blocks are mounted at the ends of the specimen. They allow frictionless movement even under an axial load of 400kN.

The experimental procedure will consist of three main steps:

1. Load the column section axially.
2. Heat the column section up to the test temperature, maintaining its axial load.
3. Load the column section transversely until failure occurs in the column web.

Tests are planned at 20°C, 450°C, 550°C and 600°C with axial load ratios of 0.0, 0.2 and 0.3. Using the reduction factors for steel yield stress given in the EC3 Part 1.2, the axial load ratios for the different temperatures are shown in Table 2.

Temperature	Reduction Factor	LR 0.0	LR 0.2	LR 0.3
	$k_{y,\theta}$	$\sigma_N / (k_{y,\theta} * f_y)$	$\sigma_N / (k_{y,\theta} * f_y)$	$\sigma_N / (k_{y,\theta} * f_y)$
20°C	1.000	0.00	0.200	0.300
450°C	0.890	0.00	0.225	0.338
550°C	0.625	0.00	0.320	0.480
600°C	0.470	0.00	0.426	0.638

Table 2 : Summary of the planned tests

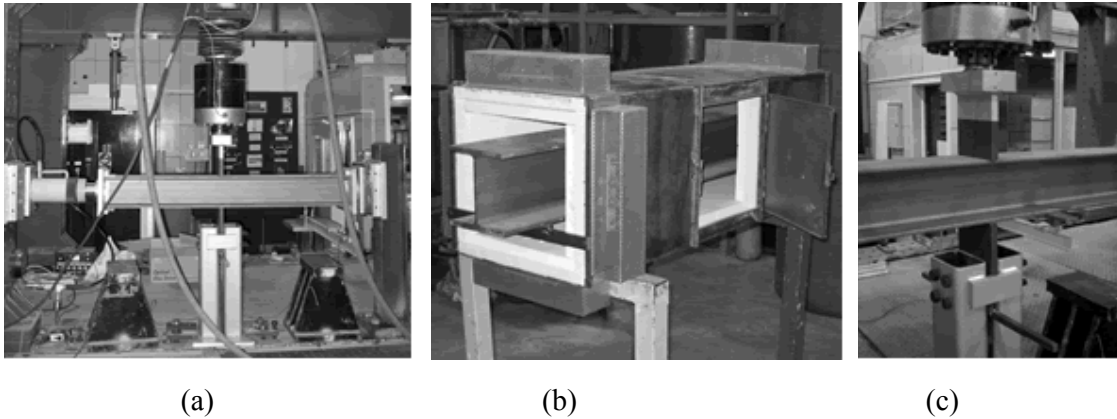


FIGURE 10 : (a) Experimental setup, (b) furnace, (c) load introduction system.

CONCLUSION

A finite element study has been performed in order to investigate the influence of the axial load in a column on its transverse compression resistance at elevated temperatures. The transverse resistance becomes important in an unstiffened beam-to-column connection if large rotations of the beam-ends in fire and thermal expansion introduce large compression forces into the column via the bottom beam flange.

From the numerical analyses a significant reduction of the ultimate transverse resistance and the displacement associated with this ultimate resistance could be seen. This is consistent with the experimental results at ambient temperatures found in the literature, but the present reduction factors for this effect are not sufficiently accurate. A new factor for the ultimate load at elevated temperatures has been developed, based on an existing approach and a large number of numerical calculations. A new reduction factor has been developed for the displacement of the ultimate load needed to be able to describe the full force-displacement

curve of the compression zone in the column web. To further validate the new reduction factors a series of high-temperature, biaxial loading experiments are planned, and the test setup is described briefly in this paper.

The compression zone in the column web is one of the major components needed to describe the full moment-rotation-thrust-temperature characteristics of steel and composite joints in fire. This knowledge will contribute to more accurate analysis of steel-framed structures in fire and thereby increase the safety and economy of structural design.

ACKNOWLEDGMENT

The authors gratefully acknowledge sponsorship of the first author by Buro Happold FEDRA Ltd, and support for the experimental work by Corus Group Ltd.

REFERENCES

- [1] European Committee for Standardization, “Eurocode 3: Design of steel structures, Part 1.8: Design of joints (Stage 49 draft)”, Document prEN 1993-1-8, (2003).
- [2] Kühnemund F., “Zum rotationsnachweis nachgiebiger knoten im stahlbau”, Dissertation, Institut für Konstruktion und Entwurf Stahl-, Holz- und Verbundbau, Universität Stuttgart, (2003).
- [3] European Committee for Standardization, “EC 3: Design of steel structures, Part 1.2: Structural fire design (Stage 49 draft)”, Document prEN 1993-1-2, (2003).
- [4] Aribert, J.M., Lachal, A. and Moheissen, M., “Modelling and experimental investigation of plastic resistance and local buckling of H or I steel sections submitted to concentrated or partially distributed loading”, Proc. IUTAM Symposium, Prague, (1990), pp.101-110.
- [5] Spyrou, S., “Development of a component based model of steel beam-to-column joints at elevated temperatures”, PhD Thesis, Department of Civil and Structural Engineering, University of Sheffield (2002).
- [6] Block, F.M., Burgess, I.W., Davison, J.B., Plank, R., (2004), “A Component approach to modelling steelwork connections in fire: behaviour of column webs in compression”, Proc. ASCE Structures Congress 2004, Nashville, Tennessee, (2004).
- [7] Lagerqvist, O., Johansson, B., “Resistance of I-girders to concentrated loads”, *J. Construct. Steel Research*, **39** (2), (1996), pp.87-119.
- [8] Zoetemeijer, P., “Influence of normal-, bending- and shear-stresses in the web of European rolled sections”, Report 6-75-18, Stevin Laboratory, Delft University of Technology, Netherlands, (1975).
- [9] Ahmed B. and Nethercot D.A., “Effect of column axial load on composite connection behaviour”, *Engineering Structures*, **20** (1-2), (1998), pp.113-128.
- [10] Bailey, C.G. and Moore, D.B., “The influence of local and global forces on column design”, Final Report, PII Contract No. CC1494, BRE, Garston, UK, (1999).
- [11] Djubek, J. and Škaloud, M., “Postbuckling behaviour of web plates in the new edition of Czechoslovak design specifications”, Proc. International Conference on Steel Plated Structures, Imperial College, London, (1976).
- [12] Tryland T., Hopperstad O.S. and Langseth M., “Finite-element modelling of beams under concentrated loading”, *Journal of Structural Engineering, ASCE*, **127** (2), (2001), pp.176-185.
- [13] Zheng, Y., Usami, T. and Ge, H.B., “Ductility of thin-walled steel box stub-columns”, *Journal of Structural Engineering, ASCE*, **126** (11), (2000), pp.1304-1311.

APPENDIX

Summary of the analysed British column sections as presented in Figs. 7 and 8:

UC Section	d / t	Temp. [°C]	Axial Load Level N / N _{pl}	Peak Load [kN]	Peak Load Reduction	Displ. at Peak Load [mm]	Displ. Reduction
203x203x46	22.30	20 C	0.00	354.89	1.00	2.17	1.00
			0.40	330.35	0.93	1.85	0.85
			0.50	315.58	0.89	1.71	0.79
			0.60	291.54	0.82	1.34	0.62
			0.70	263.54	0.74	1.19	0.55
		450 C	0.00	243.56	1.00	1.85	1.00
			0.40	209.01	0.86	1.43	0.77
			0.50	193.96	0.80	1.27	0.69
			0.60	177.67	0.73	1.17	0.63
			0.71	160.69	0.66	0.93	0.50
		650 C	0.00	92.97	1.00	1.84	1.00
			0.35	82.01	0.88	1.51	0.82
			0.50	74.17	0.80	1.26	0.68
			0.60	68.75	0.74	1.12	0.61
			0.71	62.56	0.67	0.91	0.49
			0.71	62.56	0.67	0.91	0.49
152x152x37	15.50	20 C	0.00	345.84	1.00	3.06	1.00
			0.41	309.96	0.90	2.30	0.75
			0.50	299.12	0.86	2.02	0.66
			0.60	279.24	0.81	1.79	0.59
			0.70	252.16	0.73	1.79	0.58
		450 C	0.00	238.02	1.00	2.20	1.00
			0.40	206.32	0.87	1.61	0.73
			0.51	190.48	0.80	1.45	0.66
			0.60	175.16	0.74	1.31	0.60
			0.70	157.20	0.66	1.12	0.51
		550 C	0.00	165.75	1.00	2.15	1.00
			0.40	143.72	0.87	1.61	0.75
			0.50	133.92	0.81	1.50	0.70
			0.61	120.80	0.73	1.33	0.62
			0.70	109.64	0.66	1.11	0.52
			0.70	109.64	0.66	1.11	0.52
650 C	0.00	91.22	1.00	2.37	1.00		
	0.40	78.84	0.86	1.84	0.77		
	0.50	73.60	0.81	1.70	0.72		
	0.60	67.56	0.74	1.43	0.60		
	0.70	60.96	0.67	1.19	0.50		
	0.70	60.96	0.67	1.19	0.50		
	0.70	60.96	0.67	1.19	0.50		
203x203x167	10.40	20 C	0.00	2117.56	1.00	10.29	1.00
			0.40	1955.08	0.92	8.29	0.81
			0.60	1778.94	0.84	7.31	0.71
			0.80	1536.58	0.73	6.65	0.65
		450 C	0.00	1341.85	1.00	10.65	1.00
			0.40	1189.47	0.89	6.59	0.62
			0.53	1099.03	0.82	5.68	0.53
		650 C	0.70	968.93	0.72	4.37	0.41
			0.00	519.99	1.00	10.06	1.00
			0.40	461.84	0.89	6.53	0.65